SEISMIC RESPONSE OF GRAVITY DAMS - CORRELATIONS BETWEEN SHAKE TABLE TESTS AND NUMERICAL ANALYSES

Rene TINAWI[1], Pierre LEGER[2] And Martin LECLERC[3]

SUMMARY

The purpose of this paper is to present shake table experiments conducted on four 3.4 m high plain concrete gravity dam models to study their dynamic cracking and sliding responses. The experimental results are then compared with a smeared cracked FE simulation using a nonlinear concrete constitutive model, based on fracture mechanics. For the sliding mechanism, the numerical simulations use rigid body dynamics with frictional strength derived from the Mohr-Coulomb criterion. From the cracking tests, it is shown that a single triangular acceleration pulse could initiate a crack and propagate it. For the sliding mechanism, it is shown that the cumulative sliding displacement depends on the frequency content of the seismic record. For simplified pseudo-static/dynamic sliding analyses, the concept of an *effective* acceleration is developed.

INTRODUCTION

The seismic safety of existing concrete dams is a major concern, due to the catastrophic consequences of a sudden release of the reservoir, if the dam fails under strong ground motions. Most existing dams were built many years ago with minimal consideration for seismic loads. The state of knowledge in structural dynamics and seismicity is continuously progressing such that the seismic safety of concrete dams should be periodically evaluated considering the latest assessment of their strengths and the ground motion intensity to which they might be subjected.

Guidelines for seismic evaluation of dams have been adopted in several countries. They require that, under an annual exceedance probability of 10^{-3} to 10^{-4} for a maximum design earthquake (MDE), the dam should not slide, open at joints, or crack to the extent that uncontrolled release of reservoir would take place. Although no failures have been reported, some dams have been severely damaged. In addition to historical evidences, there are also a number of shake table tests that were conducted on small scale models to predict the earthquake response of gravity dams.

On the numerical side, two different approaches have been used extensively: the discrete crack approach where remeshing of the finite element model is required, and the smeared crack approach where the mesh is fixed. In the second approach, the isotropic concrete constitutive relations are replaced with orthotropic properties. To improve mesh objectivity, the smeared crack approach introduces the tensile softening modulus related to the fracture energy of concrete, G_f, and the characteristic length of the elements (Bhattacharjee and Léger 1993).

The objectives of this work are: (i) to determine experimentally the dynamic characteristics of concrete dam models, 3.4 m high, such as natural frequencies, viscous damping, and corresponding dynamic materials properties; (ii) to perform shake table tests to determine the critical acceleration for which cracking in two monolithic dam models is observed, and to correlate the experimental cracking response with a G_f-type smeared crack model; (iii) to obtain experimentally the sliding response for two other dam models with the same height, but having an unbonded lift joint at about mid-height, and to correlate the observed cumulative displacements, due to sliding, with the results obtained from a time integration algorithm, using rigid body dynamics.

[1] *Ecole Polytechnique de Montreal, Canada*
[2] *Ecole Polytechnique de Montreal, Canada*
[3] *Ecole Polytechnique de Montreal, Canada*

More details on the historical, experimental and numerical evidence related to the seismic response of gravity dams can be found elsewhere (CEA 1998 , Tinawi et al. 1999).

DYNAMIC CRACKING RESPONSE

The design of the two specimens of a 3.4 m dam model with a thickness of 0.25 m is shown in Fig. 1. To reduce the natural frequency, a 2700 kg mass was anchored at the crest. This mass is not representative of a real dam but was necessary to obtain experimentally a reasonable dynamic amplification of the dam model. The compressive strength of concrete was 15MPa, typical of older gravity dams. To control the location of crack initiation, two notches 10 mm thick and 250 mm long were introduced on the upstream and downstream faces of the model. These notches, located 1m above the footing, decreased the natural frequency of the specimens to 16.4Hz using the FE model shown in Fig. 2. The total mass of the specimen, including the added mass at the crest, was 6800 kg. Viscous damping for the monolithic specimens was measured. This resulted in a value of 0.9% for the first specimen, as shown in Fig. 3. For the second specimen, the measured damping value was 1.3%.

The two monolithic specimens were subjected to simple acceleration pulses to observe their cracking responses. Simple pulses are easier to use and interpret compared to seismic records. The total duration of the pulse is 0.1 sec and is made up of two triangular acceleration segments, one positive and the other negative. There is a difference between the laboratory input and the measured acceleration at the base of the specimen. This difference stems from the presence of high inertia loads on the shake table, the short duration of the pulse and the performance of the shake table.

The first monolithic specimen was then subjected to triangular acceleration pulses. The first peak acceleration (FPA) was increased progressively in approximate increments of 0.1g. Up to an FPA level of 0.87g no cracking was observed as shown in Fig. 4(a). By increasing further the acceleration level, a partial crack was observed at a FPA = 0.94g (Fig. 4(b)). This partial crack initiated on the downstream face, at the notch level, with an initial angle of about 30° downwards and propagated, at an average velocity of 35 m/s, about 350 mm as shown in Fig. 4(b). Advantage was taken of this situation to measure the natural frequency and the viscous damping. Figure 3 shows a lower natural frequency of 13.3 Hz and a damping ratio of 23%. This rather high value for the viscous damping includes localised intergranular frictional effects as well as energy dissipation due to impact upon closing of the crack. However, such localised effects are not considered in the present FE model and are subject to large variations as the crack propagates through the dam model. Care and judgement must be exercised prior to using high damping values in practice. By attempting to repeat the last acceleration level input, the crack extended fully in a near horizontal plane, to reach the other notch (Fig. 4(c)) at a FPA= 0.98g.

The second homogeneous specimen was tested with the objective to determine the influence of subsequent pulses, over the first, on the crack propagation. From Fig. 4(d) it is observed that three consecutive pulses with a FPA of 0.96g were sufficient to fully crack the dam into two separate bodies. For the tests shown in Fig. 4, the observed extent and direction of the crack correlate fairly well with the smeared rotating crack model used in FRAC-DAM (Bhattacharjee 1996). This smeared crack model based on nonlinear fracture mechanics principles is used to represent crack initiation and propagation. The development of the constitutive model relies on an energy-based softening initiation criterion, fracture energy conservation during the damage process, closing and opening of the crack during cyclic excitations, shear deformations in the fracture process zone and the subsequent rotation of the crack planes. Details of the model are given in Bhattacharjee and Léger (1993). The material parameters are the fracture energy G_f, the tensile strength f_t, and the slope of the post peak response.

Figure 5 presents comparisons between the second cracking test of the first monolithic (now pre-cracked) specimen and numerical simulations. Since partial cracking leads to a viscous damping value of 23%, this value could be considered as new input for the second crack test. However, when using this equivalent viscous damping ratio, derived from low amplitude impact tests, both the local (CMOD) and the crest relative displacement responses are grossly underestimated under a seismic pulse excitation. This confirms the localised influence of the crack, which should be simulated by local frictional elements and local dampers. In fact, when the CMOD reaches a value of about 1.2 mm, the specimen is fully cracked. During the cracking process of the specimen, the viscous damping changes significantly but this variation is not considered by FRAC-DAM. A damping value of 10% appears to reproduce better the experimental results. Finally, the high viscous damping value of 23% was experimentally derived from impact tests where the specimen experienced global energy dissipation through many cycling motions and impacts, which are not induced during this short base motion testing of 0.1 s in duration.

Figure 6 presents comparisons between the cracking test of the second homogeneous model, subjected to three pulses, and numerical simulations using 1.3% viscous damping. As observed in the first monolithic specimen, the cracking sequence is the same. It corresponds to two consecutive openings at the downstream notch (at 0.05 s and at 0.14 s). However, the second opening, in this case, leads to the complete cracking of the specimen due to the second pulse. Yet, its stability after complete cracking was not of concern during the third pulse. The first experimental opening of 0.12 mm, which corresponds to the crack initiation, was measured at 0.05 s. In the numerical model, the value of the fracture energy that yielded the best fit with the observed CMOD was 54 N.m/m² and is within 10% of the value suggested by the CEB-FIP prior to dynamic amplification which was 1.75. Although the specimen is fully cracked after 0.15 s, numerical analyses reproduce well the observed dynamic response. This is due to the fact that in the FE analysis at least one element always remains under compression thus ensuring contact.

DYNAMIC SLIDING RESPONSE

Two specimens with a cold lift joint, introduced 1m above the footing, by casting the lower part of the specimen separately from the upper part, were constructed as shown in Fig. 7. In fact, the lower part of the joint was cast and cured in a vertical position for three days before casting the upper part. The main objective of these experiments is to study the sliding behavior under quasi-static and dynamic loads. To avoid rocking of the upper block, the 2700 kg crest mass used earlier, during the cracking tests, was removed. However, to induce downstream sliding, a horizontal force is introduced with a 700 kg hanging mass attached to the upstream face of the specimen with a cable. The cable location on the upstream face was placed close to the joint level to avoid potential rocking of the upper block. The cable stiffness was selected to minimise the dynamic amplification of the suspended mass with that of the upper block. The experimental set-up allowed several sliding tests to be carried out for each specimen by simply replacing the upper block to its original position after sliding.

To break the bond at the joint location, a 10 Hz sinusoidal acceleration, with increasing amplitude, was used for the first specimen. Failure and subsequent sliding occurred at 2.1g. For the second specimen, failure of the joint was obtained using the Chicoutimi North transverse record (PGA=0.13g) of the 1988 Magnitude (M_s) 5.7 Saguenay earthquake (Mitchell et al. 1990). Failure and subsequent sliding occurred when the PGA was increased to a value of 0.5 g. This lower PGA value is due to the pre-damage of the joint. Static tests, on both specimens, to obtain the coefficient of friction yield a value for $\mu = 0.68$ for the peak response, and $\mu = 0.6$ for the residual response.

The critical acceleration must be overcome for sliding to occur. The value of the critical acceleration, a_{cr}, is:

$$\frac{a_{cr}(t)}{g} = \mu - \frac{F(t)}{Mg} \tag{1}$$

In general, when there is no cable force, F(t), the critical acceleration is equal to μ. However, this value is reduced due to the presence of the cable force. If F(t) is assumed constant, the downstream critical acceleration is 0.0615g. The upstream critical acceleration is 1.14g. This means the upper block can only move downstream. The value M of the sliding block is 1300 kg.

Figure 8 shows the sliding response of the second specimen with a joint, submitted to the 1988 Saguenay record scaled to a PGA = 0.53g and the 1940 El Centro (S00E component) record scaled to 0.28 g. The numerical simulation using the Saguenay record correlated well with the experimental test using a constant value ($\mu = 0.6$) for the friction coefficient. However, the numerical simulation using the El Centro record overestimated the experimental sliding response, when using $\mu = 0.6$. In this case, non-negligible rocking rotations (around 0.1°) occurred during the experimentation. These rotations always occurred before sliding thus creating a vertical acceleration component, which increased the vertical forces acting on the upper block during sliding initiation. Since the development here does not consider rocking, a higher value for the friction coefficient was used to correlate with the experiment for low frequency ground motions.

The Saguenay record with a PGA increased to 0.53g produced experimentally sliding displacements of the order of 93 mm only. The El Centro earthquake with a PGA scaled down to 0.28g produced experimental sliding response of the same order (123 mm). Therefore, the frequency content and the duration of a seismic record affect significantly the cumulative sliding response.

EFFECTIVE ACCELERATION TO INDUCE SLIDING

From equation (1) the critical acceleration is presented as a function of F(t) which implies that a_{cr} is a function of time. In real situations, the main static force acting on the dam is the hydrostatic pressure, which is constant, and the hydrodynamic effect is often assumed as an added mass. In this case, a_{cr} is not a function of time.

If the cable force during the experiments is assumed constant, with a value of 700 kg x 9.81 m/s² = 6867 N, the critical accelerations, corresponding to various values of μ, can be obtained. An arbitrary limit for the sliding, s_{lim}, is set at 1 mm such that sliding below this value is not of structural significance. For example, for μ=0.65, the acceleration A_1, required from a transient analysis to produce a sliding with a value of s_{lim}, is 0.24g while the corresponding a_{cr} value is 0.112g. In a pseudo-static or pseudo-dynamic sliding analysis an "effective" acceleration of 0.112g, for which the sliding safety factor is one, will therefore induce the sliding displacement s_{lim} for the Saguenay record at a PGA level of 0.24g. The pseudo-static "effective" acceleration is thus defined as $A_{eff}= \lambda$ (PGA) where λ is the ratio a_{cr}/A_1. For the El-Centro record a lower bound for λ can be estimated at 0.67 while for the Saguenay record, typical of Eastern earthquakes, the lower bound for λ is 0.5 (Tinawi et al. 1999).

CONCLUSIONS

Shake table tests have been carried out on two 3.4 m high concrete dam models to provide information on the cracking response when subjected to simple triangular acceleration pulses. The other two specimens had cold joints that were allowed to slide after breaking them. Sliding tests included North American eastern (high frequency) and western (low frequency) acceleration records. The tests correlated well with the numerical procedures and provided an opportunity to investigate the robustness of existing software. A single triangular acceleration pulse can cause partial cracking in a concrete dam. Two consecutive pulses did cause complete cracking. The material properties of concrete were increased by a constant dynamic magnification of 1.75 to obtain a good correlation. Even if viscous damping for the uncracked model increased significantly after cracking, it is not recommended, at this time, to exceed a viscous damping value of more than 10%.

Sliding displacements due to eastern or western North American earthquake records confirm the importance of the frequency content of the accelerograms. Good correlation with experimental results was obtained using numerical simulations based on rigid body dynamics and frictional strength limited by Mohr-Coulomb criterion. The experimental sliding responses and numerical analyses of the models indicate that the concept of *effective* acceleration, A_{eff}, is appropriate for pseudo-static or pseudo-dynamic analyses. From this study, the pseudo-static effective acceleration for high frequency eastern North-American earthquakes can be estimated as 0.5 PGA, and 0.67 PGA for low frequency western earthquakes.

REFERENCES

Bhattacharjee, S. (1996). "FRAC_DAM a finite element analysis computer to predict Fracture and Damage responses of solid concrete structures", Dept. Civil Eng., *Report No. EPM/GCS 1996-03*, École Polytechnique de Montréal, Canada.

Bhattacharjee, S. and Léger, P. (1993). "Seismic cracking and energy dissipation in concrete gravity dams". *Earthquake Engineering and Structural Dynamics*. Vol.22, 991-1007.

CEA. (1998). Canadian Electricity Association. "Structural safety of existing concrete dams -Influence of construction joints. Final Report"; Volume A – "Review of the literature and background material", and Volume B – "Theoretical and numerical development and case studies". *CEA Report No. 9032 G 905*, prepared by École Polytechnique, Montréal, Canada.

Mitchell, D., Tinawi, R. and Law, T. (1990). "Damage caused by the November 25, 1998 Saguenay earthquake". *Canadian Journal of Civil Engineering.* Vol. 17 (3), 338-365.

Tinawi, R., Léger, P., Leclerc, M. and Cipolla, G. (1999). "Seismic safety of gravity dams: From shake table experiments to numerical analyses". *ASCE Journal of Structural Engineering.* In press.

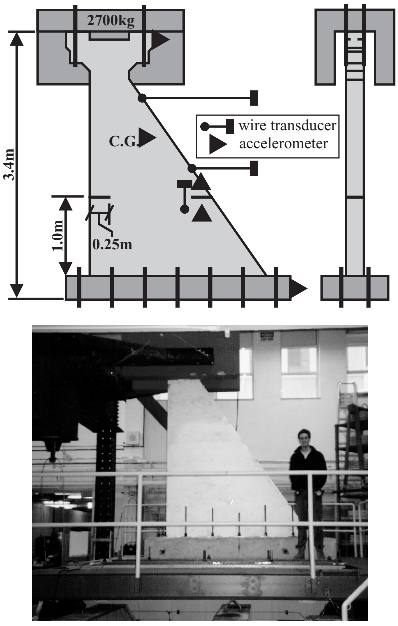

Figure 1: Monolithic dam model and instrumentation setup.

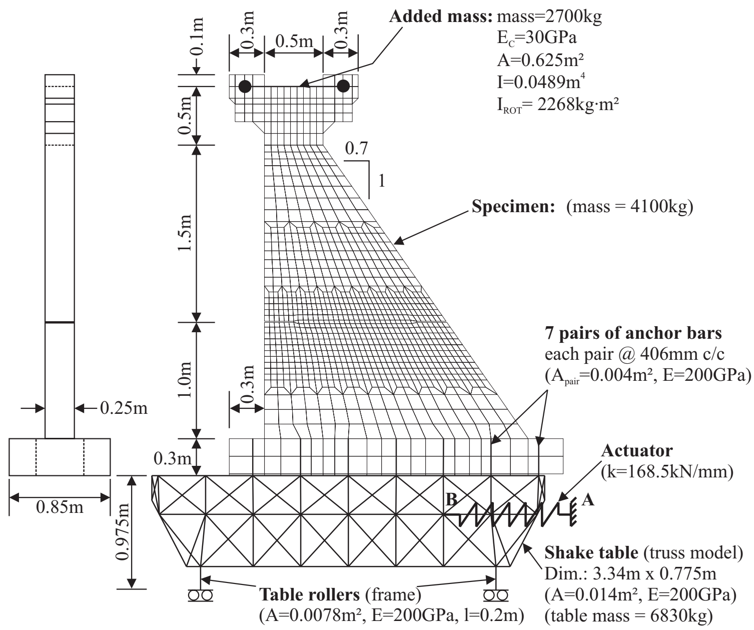

Figure 2: Finite element model with shake table and actuator.

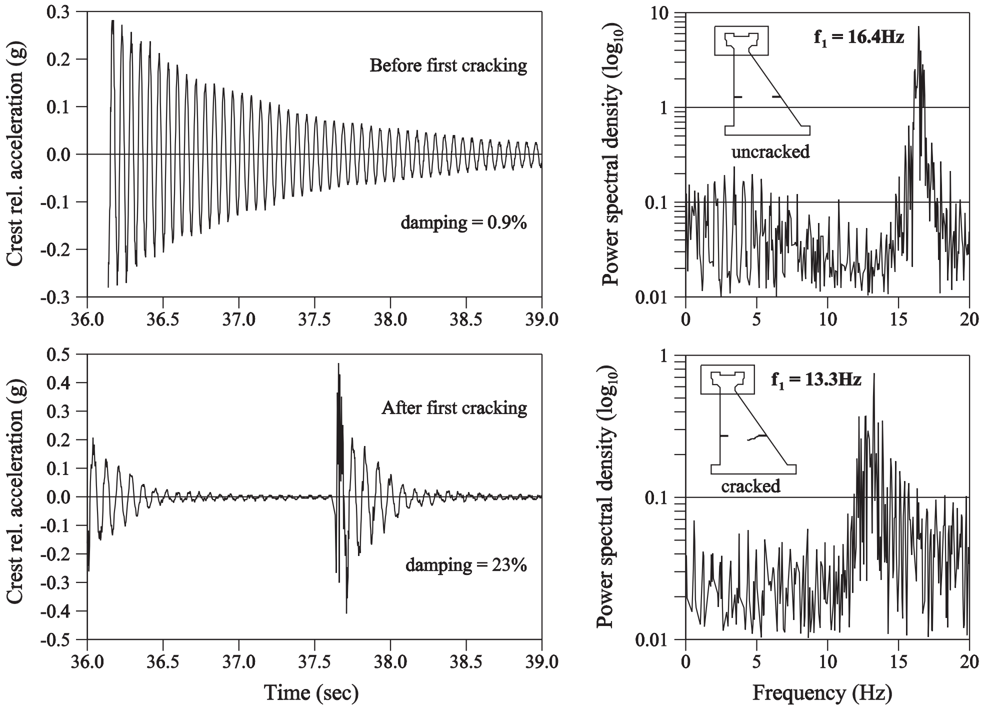

Figure 3: Laboratory impact tests before and after the first cracking of the first monolithic specimen.

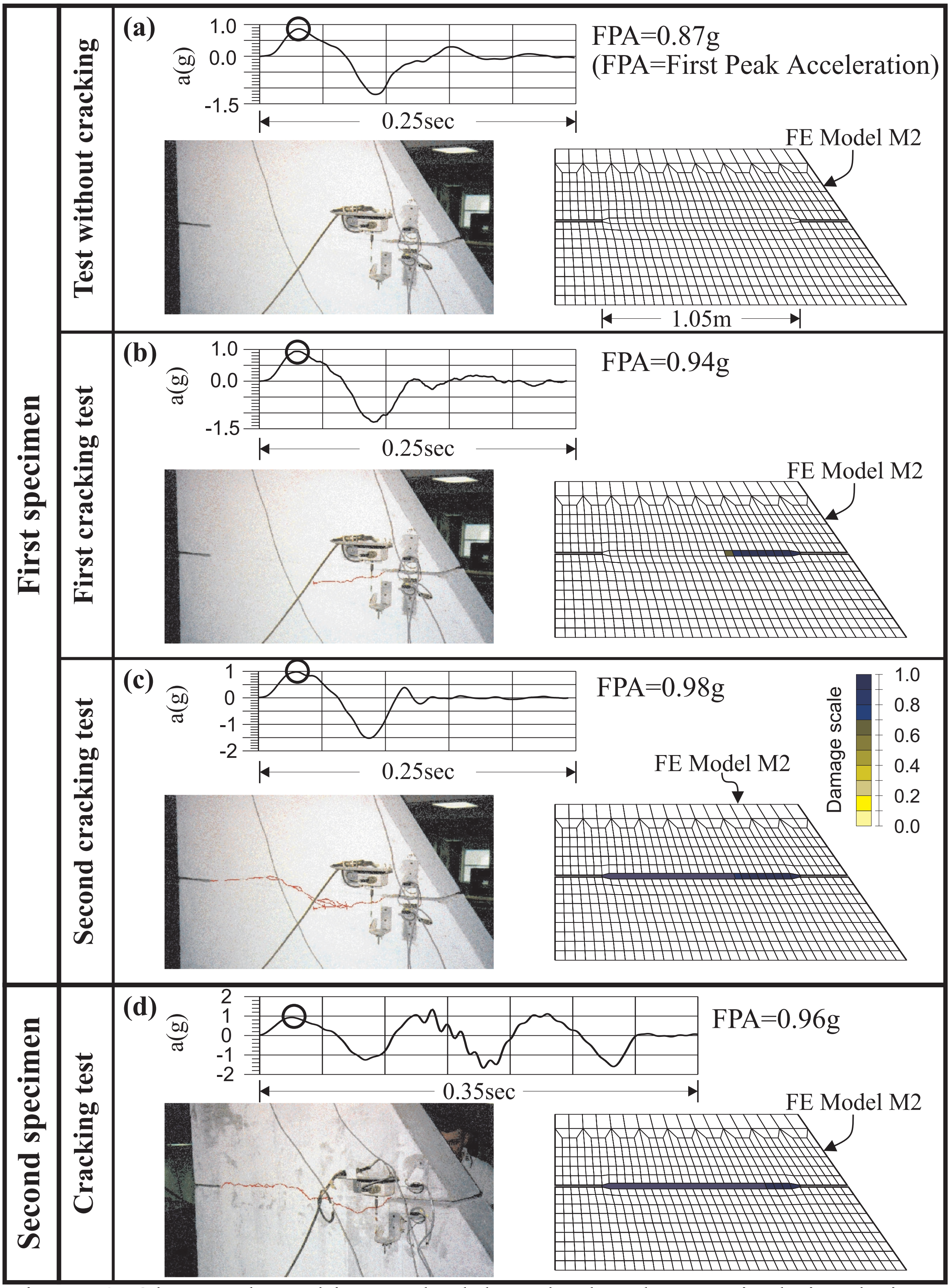

Figure 4: Observed cracking at the lab and related numerical simulations.

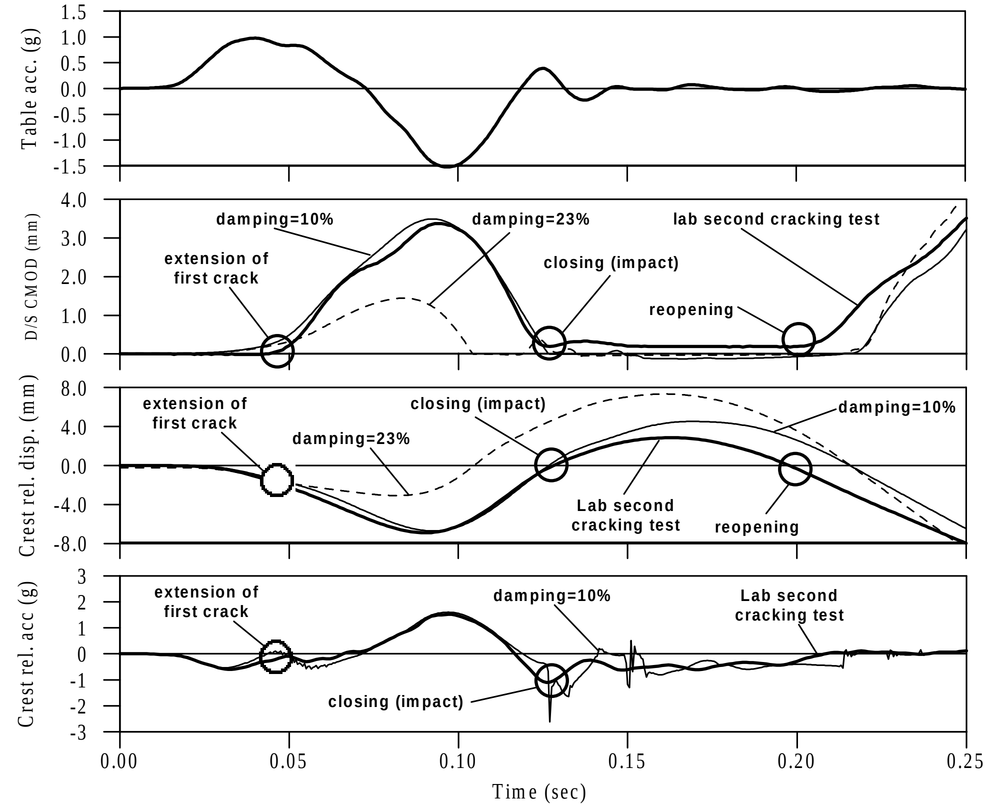

Figure 5: Comparisons between the second crack test of the first monolithic specimen and numerical simulations using the FE model M2 with different damping ratios.

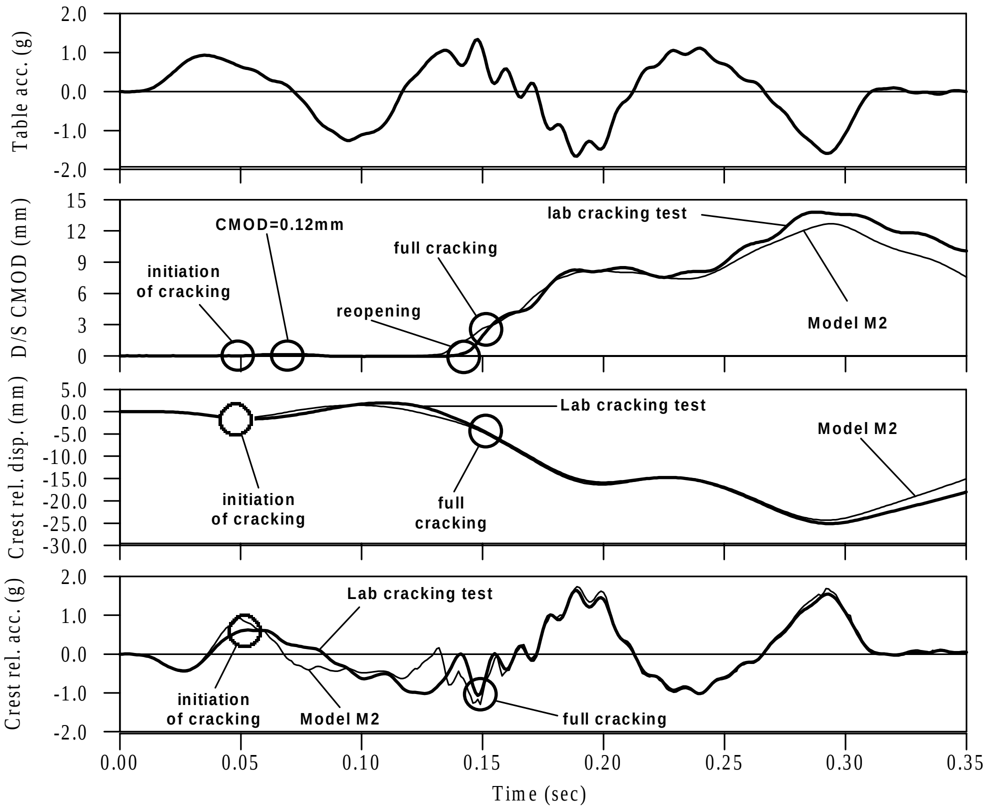

Figure 6: Comparison between the cracking test of the second monolithic specimen and numerical simulations using the FE model M2 (viscous damping=1.3%).

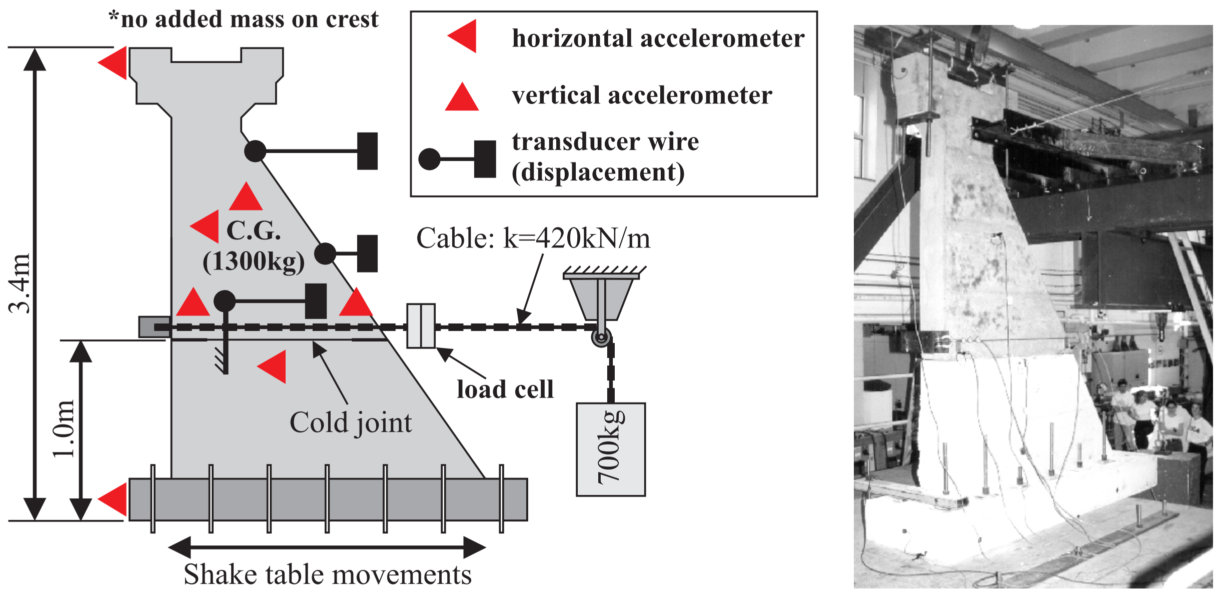

Figure 7: Instrumentation and experimental setup for the dam model with a cold joint.

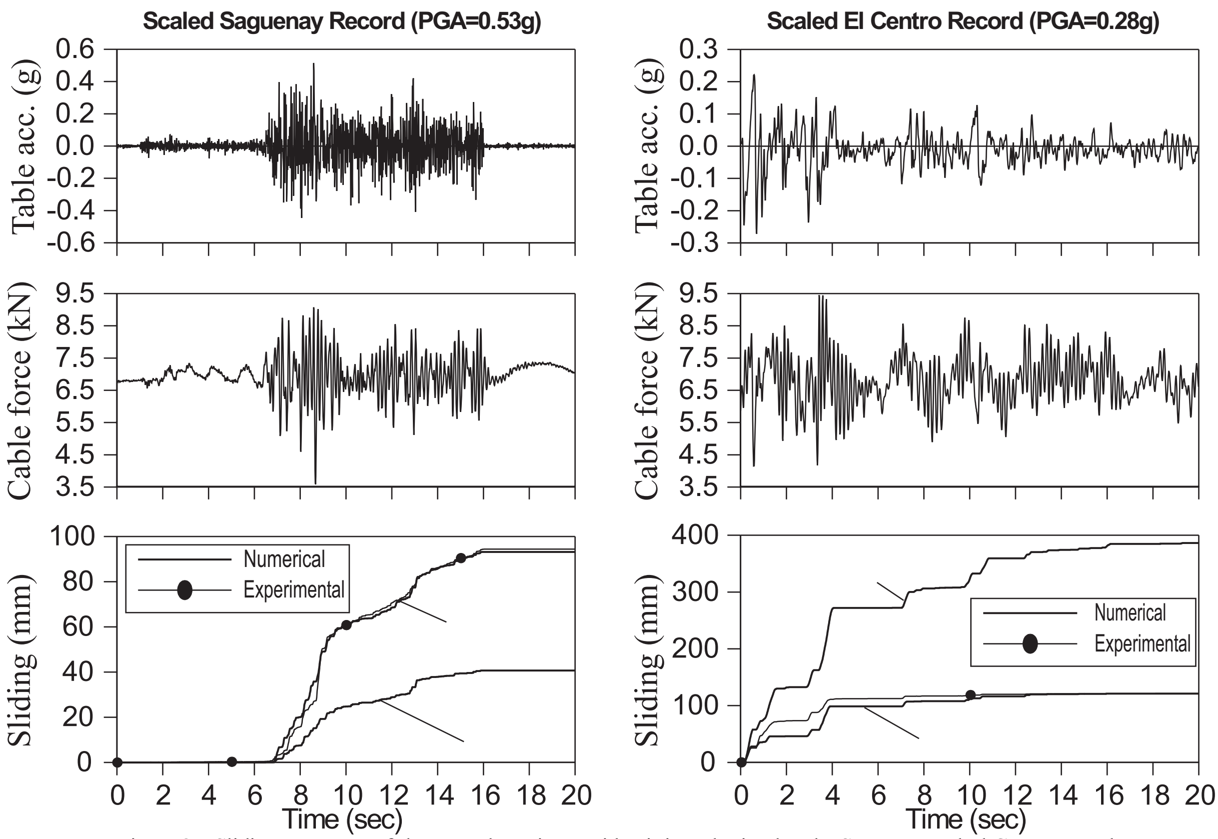

Figure 8: Sliding responses of the second specimen with a joint submitted to the Saguenay and El Centro records.